Published in final edited form as:
Neurosci Lett. 2008 February 6; 431(3): 191–196.

Crossmodal Propagation of Sensory-Evoked and Spontaneous Activity in the Rat Neocortex

Kentaroh Takagaki[1], **Chuan Zhang**[1], **Jian-Young Wu**[1], and **Michael Thomas Lippert**[2]

1*Department of Physiology and Biophysics, Georgetown University, Washington, DC 20057*

2*Leibniz-Institute for Neurobiology; 39118 Magdeburg; Germany*

Abstract

In the cortex, neural responses to crossmodal stimulation are seen both in higher association areas and in primary sensory areas, and are thought to play a role in integration of crossmodal sensations. We used voltage-sensitive dye imaging (VSDI) to study the spatiotemporal characteristics of such crossmodal neural activity. We imaged three cortical regions in rat: primary visual cortex (V1), barrel field of primary somatosensory cortex (S1bf) and parietal association area (PA, flanked by V1 and S1bf). We find that sensory-evoked population activity can propagate in the form of a distinct propagating wave, robustly in either crossmodal direction. In single trials, the waveforms changed continuously during propagation, with dynamic variability from trial to trial, which we interpret as evidence for cortical involvement in the spreading process. To further characterize the functional anatomy of PA, we also studied the propagation of spontaneous sleep-like waves in this area. Using a novel flow-detection algorithm, we also detected a propagation bias within PA of spontaneous waves—these tend to propagate parallel to the crossmodal axis, rather than orthogonal to it. Taken together, these findings demonstrate that intracortical networks show pre-attentive crossmodal propagation of activity, and suggest a potential mechanism for the establishment of crossmodal integration.

Keywords

voltage-sensitive dye imaging; spatiotemporal patterns; flow analysis; propagating waves; spontaneous activity

Introduction

Combining input from several modalities can improve perception and behavior [38]. Recent findings in human imaging have directed attention to multisensory responses in the early stages of cortical processing [7,8]. Crossmodal influences in early cortical stages have been observed in humans [8,11,13,22,24,27], nonhuman primates [4,17,21,36,37], cats [1], ferrets[5], and rodents [25,40]. Such widespread observations of multisensory responses in sensory cortex has lead to the proposal that all “unisensory” areas may indeed encompass multisensory characteristics [9,12,35], especially when measures sensitive to subthreshold activity such as

Corresponding author: Kentaroh Takagaki, Department of Physiology and Biophysics, Georgetown University, WP26 Research Building, 3970 Reservoir Road, NW, Washington, DC 20007, Phone: +1-202-687-1617, Fax: +1-202-687-0617, kt62@georgetown.edu.

evoked potentials [6,25], but also in unit activity [40]. Little is known, however, of how this neural activity manifests spatiotemporally on the population level.

Crossmodal transmission of activity may potentially be observed with voltage-sensitive dye imaging (VSDI), as has been predicted previously [31]. This technique measures activity in cortical surface layers, and mainly reflects dendritic postsynaptic potentials [32]. In this study, we directly tested whether it is possible to capture crossmodal transmission of neural activity with voltage-sensitive dye imaging. In particular, we tested the hypothesis that modality-specific activation is followed by the spread of this activation to surrounding non-specific areas, in the form of propagating waves of population activity [10].

Materials and Methods

Surgery

Eleven adult Sprague Dawley rats (250 – 400 g) were used. Surgical procedures were approved by Georgetown University Animal Care and Use Committee following NIH guidelines. For details, see Lippert, et. al., 2007 [23].

Briefly, animals were pretreated with atropine sulfate (40 μg/kg IP) and xylazine (2 mg/kg), intubated via tracheostomy, and ventilated with isoflurane in conditioned room air. End-tidal carbon dioxide ($ETCO_2$) was maintained at 3.4–3.6%. Anesthesia was closely monitored, and supplemented with additional xylazine. Physiological support included maintenance of normothermia, infusion of Ringer solution (approx. 2.5 ml/kg/hr SQ), and application of bland ophthalmic ointment. Cranial windows were drilled over visual cortex (bregma −4 to −9 mm, lateral 1 to 6 mm), barrel field (bregma −0 to −5 mm and lateral 2 to 7 mm), or parietal association area (bregma −2 to −7 mm and lateral 1.5 to 6.5 mm). Voltage-sensitive dye RH-1691 (Optical Imaging) was applied transdurally (2 mg/ml in ACSF), for 1.5 to 2 hr. After staining, excess dye was rinsed for >15 min.

Imaging

Imaging utilized a macroscope with large numerical aperture [19,23]. Excitation light was filtered at 630 ± 15 nm and reflected onto the cortex via a 655 nm dichroic mirror. Signal was filtered through a 695 nm long pass filter and projected onto the aperture of a 464-channel hexagonally packed photodiode array. Each detector of the array received light from an area of approximately 160 μm in diameter, and was individually amplified. Neuroplex (RedShirtImaging) was used to coordinate data acquisition, at 1.6 kHz. An ECG-triggered subtraction algorithm was used to subtract heartbeat artifact, when present [23]. All data presented were recorded in single trials, without averaging. For frame images, a 7-tap hexagonal spatial filter (nearest neighbors) was applied. Traces were filtered between 1–100 Hz for display. Custom programs were used (Java/Mathematica), and are available upon request.

For visual stimulation, a white LED was positioned in front of the contralateral eye. The visual stimulus lasted for 10 ms and covered approximately 40° of the visual field of the animal. The stimulus light path was shielded to avoid contamination of the optical recordings. For whisker stimulation, we used a 200 ms ramp-and-hold deflection to whisker alpha, in the anterior direction, delivered via a modified galvanometer providing rapid deflections of 3 mm (~15°). Other whiskers were cut off to prevent inadvertent stimulation.

Flow Field Calculation

Our flow-field calculation is based on time-shifted correlations between detector pairs in the field, and is described in detail in the supplemental material. Briefly, if two waveforms from

neighboring detectors show high correlation with each other with a certain temporal delay, this delay can be taken as a measure of propagation speed between these neighboring detectors (Supplemental Figure 2A). The two-dimensional flow for a given detector can be calculated by isotropic aggregation of this measure for neighboring pairs (Supplemental Figure 2B). We used a correlation window of 100 ms (160 frames); windows of 75 ms and 150 ms yielded similar results (data not shown). We calculated the following metrics for each detector: flow direction, flow velocity, and flow reliability (i.e. the average correlation coefficient of all pairs sampled). Detected events with flow reliability lower than 0.9 were discarded.

Results

Crossmodal Propagation of Sensory-Evoked Activity Between Visual and Somatosensory Cortex

We expected crossmodal propagation of population activity to be low in amplitude, and theferore tested under conditions where a large population of spatially proximal neurons is activated synchronously, to facilitate voltage-sensitive dye imaging [14]. Namely, we used higher concentration isoflurane anesthesia (≥ 1.5 % isoflurane). Evoked activity was recorded with voltage-sensitive dye imaging in three fields: primary visual cortex (V1), barrel field of primary somatosensory cortex (S1bf) and parietal association area (PA) (Figure 1A). PA is abutted spatially by S1bf and V1, and has shown crossmodal responsivity in electrical recording studies [40]. Each field was imaged in independent experiments, both because we failed to attain physiological stability with larger craniotomies, and because the curvature of the rat brain prohibits simultaneous imaging of all three fields in totality. Subsequent quantification was based on images centered on the PA (e.g. red hexagon in Figure 1A), which included significant portions of both V1 and S1bf.

Under these conditions, we observed a robust and spatiotemporally coherent wave of sensory-evoked activity between V1 and S1bf (Figure 1C). Visual flash stimulus resulted in activity propagating from V1 through PA to S1bf (Figure 1C, “F”), whereas somatosensory whisker stimulus evoked the reverse pattern (Figure 1C, “W”). Under these anesthetic conditions, all recording trials (flash, n=156 trials, whisker, n=156; 8 animals) without spontaneous activity within 500 ms prior to stimulus presentation (i.e. preceding activity was <25% of maximum) showed such robust crossmodal propagation, resulting in propagating activity similar to the representative trials shown in Figure 1C. Crossmodal propagation was defined as propagation of a waveform initiating at a detector within the modality-specific area (within 100 ms of stimulus onset), and showing correlation with waveforms in proximal detectors, thus transmitting continuously into the non-specific area. No waveforms jumped detectors at the scale of observation (i.e. no waveforms showed correlation between two remote detectors but not in the detectors between them).

This crossmodal propagation was bidirectional, but asymmetric, as illustrated for representative trials (Figure 2). In order to better visualize the trial-to-trial variability and asymmetry of this crossmodal propagation, we created linescans by selecting a single row of detectors from the imaging field along the crossmodal axis (approximately parallel to the anterior-posterior axis), and plotting the normalized signal from each detector as a function of time [3] (Figure 2C–E). The flash caused V1 activity (latency 39.8 ± 2.6 ms) which generally invaded PA rapidly (latency 47.93 ± 11.0 ms), but showed a variable delay before propagating into the S1bf (latency 118.9 ± 36.7) (Figure 2C,Supplemental Figure 1B). This delay is manifested as the elongated horizontal section within the linescan (broken arrow in trial 1). This pattern resembles that seen at the rat V1/V2 border [41]. Whisker deflection caused activity in S1bf with less latency (14.6 ± 2.1 ms). This activity spread in the reverse direction into V1 with no clear delay within the PA area (Figure 2D, broken arrow, and Supplemental Figure 1B) into S1bf (latency 112.3 ± 42.2). When stimuli were applied simultaneously, the

resulting spatiotemporal pattern was altered, and did not present as a linear sum of the two independent patterns (Figure 2E, Supplemental Figure 1A). For example, longer-latency crossmodal components were absent with simultaneous stimulation (Figure 2E, Supplemental Figure 1A).

Crossmodal Propagation of Spontaneous Activity

Recent studies suggest that spontaneous patterns of population activity in visual cortex may encapsulate underlying spatial patterns of sensory processing networks [18]. We predicted that this may also hold true for interareal organization. Namely, if the sensory-evoked crossmodal propagation that we observe reflects a cortical processing pathway, spontaneous activity may also favor this type of propagation. To test this hypothesis, we quantified the propagation of spontaneous sleep-like waves recorded within segments of our data prior to stimulation, under lighter isoflurane anesthesia (≤ 1% supplemented with xylazine) [23]. A tendency for propagation in the crossmodal direction would suggest an adaptation of the underlying circuitry to support preferential propagation in this cortical axis.

In order to measure the propagation direction of spontaneous waves, we first developed an algorithm to quantify wave propagation (see Experimental Procedures, Supplemental Experimental Procedures, and Supplemental Figure 2 to Supplemental Figure 4). Previous analytical methods of optical data rely mainly on areas of activation in multi-trial averages [33, 42], and thus do not take into account the waveform data from single detectors. Furthermore, these methods give global geometrical metrics, and are not suited for characterizing the spatial distributions of function in local areas of cortex.

We applied this method with a sliding window of 100 ms, and detecting only events where the average correlation coefficient (“flow reliability”) within each calculation field exceeded 0.9. The result of this analysis for a representative experiment is demonstrated in Figure 3. Spontaneous events were detected for the selected detectors in PA (yellow detectors in Figure 3A and 3B). All of the spontaneous events from these detectors were plotted in Figure 3C (in this dataset, data for ~1 min of spontaneous activity was analyzed, and an average of ~280 events were detected for each of the 21 detectors chosen). The speed distribution of these events, regardless of the direction, is shown in the normalized histogram in Figure 3E, in yellow. The direction distribution of these events, regardless of the speed, is shown in the normalized rose histogram in Figure 3F, also in yellow. For comparison, similar data from the center of the barrel cortex (overlying barrel C2) is also displayed in Figures 3D, 3E (white), and 3F (white). PA spontaneous waves (Figure 3E, yellow) were significantly slower than S1bf spontaneous waves (Figure 3E, white) (0.200 [m/s] vs. 0.322 [m/s]; Wilcoxon rank sum test, $p<10^{-6}$). Moreover, whereas spontaneous waves from inside the barrel cortex showed no significant bias in the distribution of directions, spontaneous waves within PA showed a clear preference for propagation within the crossmodal axis (Figure 3F). A Kruskal-Wallis nonparametric ANOVA showed high significance for the propagation bias ($p<10^{-6}$), when comparing the anterior, posterior, medial and lateral quadrants in Figure 3F (indicated by yellow dashes). All animals showed similarly strong bias. This result suggests that the two primary sensory areas are coupled preferentially, even in the absence of sensory input. In order to demonstrate this finding qualitatively, we have also compared single detector traces of data (Supplemental Figure 5).

Discussion

We report that crossmodal neural activity can propagate in the form of propagating waves of population activity between V1 and S1bf. Propagating waves recorded with voltage-sensitive dye imaging can represent suprathreshold as well as subthreshold activity [31], but findings in electrophysiology suggest that our crossmodally propagating waves likely reflect network

population patterns of subthreshold, modulatory activity [1]. Combined with the aforementioned reports, our results suggest that wave-like propagation of population activity may be one correlate of crossmodal information transmission.

Such propagating waves as we observe may have several mechanisms [10]. Anatomically speaking, they may have subcortical (thalamic) mechanisms, intracortical mechanisms, or both. While our experimental design can not fully distinguish between these possibilities, several properties of the phenomena suggest cortical involvement. First, the timing and propagation velocities of these waves are variable from trial to trial (Figure 2,Supplemental Figure 1A), which suggests intracortical propagation rather than a patterned sequence of thalamic relay input. Second, the response to simultaneous crossmodal stimulation is spatiotemporally quite distinct from stimulation of each modality independently (Figure 2E,Supplemental Figure 1A), suggesting complex intracortical interactions [39]. Third, the voltage-sensitive dye signal originates, as mentioned previously, in the surface layers (mainly layers II/III) of the rat cortex, reflecting both suprathreshold and subthreshold activity [19, 23,31]. These layers receive predominantly intracortical input, and support intracortical lateral transmission of population activity [20,39]. Direct anatomical projections between visual and somatosensory cortex in rat have also been documented [26,30]. Fourth, the waveforms change continuously as they propagate, which suggests a strong intracortical component [34]. Fifth, the amplitude of these propagating waves did not decline suddenly at the areal borders, which demarcate area-specific thalamic projection patterns (Figures 2A, 2B). However, “non-specific,” diffuse thalamic afferents projecting to the supragranular layers [16] may also play a role—indeed, for some crossmodal local field responses, timing suggests this to be the case [21]. Since our waves show a larger crossmodal delay (118.9 ± 36.7 ms from V1 to S1bf, 112.3 ± 42.2 ms from S1bf to V1) and clear spatiotemporal organization, they may be mechanistically distinct from this local field response. Sixth, we observe a congruent crossmodal transmission bias even in spontaneous sleep-like waves, the bias oriented in an axis connecting the two neighboring sensory areas (Figure 3).

Flash-evoked and whisker-evoked activation showed asymmetric spatiotemporal patterns (Figure 2C and 2D). Experiments in other species have also suggested asymmetry in crossmodal influence [17, 28, 29]. Such inequalities may be a manifestation of individual stimulus characteristics, and the types of neural activity that they evoke. For example, the waves evoked by stimulation of a single whisker have a discrete point source, which is limited to the somatotopic barrel [23], and may therefore have more favorable propagation characteristics than waves evoked by a full-field flash, which diffusely activates the whole V1 almost instantaneously [23]. Crossmodal asymmetry may also be a manifestation of anisotropies in global anatomical projections [15, 26] or local coupling of the underlying network [10], both of which should be modifiable through developmental deprivation schemes or training. Further experiments will explore these matters.

In summary, we demonstrate robust feed-forward propagation of population neural activity between visual and somatosensory cortices, observed with single-trial voltage-sensitive dye imaging (VSDI) [2,23]. Furthermore, we demonstrate that even in the absence of sensory stimulation, spontaneous sleep-like waves tend to propagate parallel to the crossmodal axis, rather than perpendicular to the crossmodal axis. Taken together, our results support the hypothesis that crossmodal propagation of neural activity, in the form of propagating waves of activity [10], may contribute to multimodal responses in primary sensory areas.

Supplementary Material

Refer to Web version on PubMed Central for supplementary material.

Acknowledgments

We would like to thank Drs. Cristoph Kayser, Afonso Silva, Hongtao Ma, Xiaoying Huang, and Sunbin Song for critical reading of this manuscript. This work was supported by NIH NS36447 to JYW.

References

1. Allman BL, Meredith MA. Multisensory Processing in 'Unimodal' Neurons: Cross-Modal Subthreshold Auditory Effects in Cat Extrastriate Visual Cortex. J. Neurophysiol. 2007
2. Arieli A, Shoham D, Hildesheim R, Grinvald A. Coherent spatiotemporal patterns of ongoing activity revealed by real-time optical imaging coupled with single-unit recording in the cat visual cortex. J. Neurophysiol 1995;73:2072–2093. [PubMed: 7623099]
3. Bao W, Wu JY. Propagating wave and irregular dynamics: spatiotemporal patterns of cholinergic theta oscillations in neocortex in vitro. J. Neurophysiol 2003;90:333–341. [PubMed: 12612003]
4. Benevento LA, Fallon J, Davis BJ, Rezak M. Auditory--visual interaction in single cells in the cortex of the superior temporal sulcus and the orbital frontal cortex of the macaque monkey. Exp. Neurol 1977;57:849–872. [PubMed: 411682]
5. Bizley JK, Nodal FR, Bajo VM, Nelken I, King AJ. Physiological and Anatomical Evidence for Multisensory Interactions in Auditory Cortex. Cereb. Cortex. 2006
6. Brett-Green B, Fifkova E, Larue DT, Winer JA, Barth DS. A multisensory zone in rat parietotemporal cortex: intra- and extracellular physiology and thalamocortical connections. J. Comp. Neurol 2003;460:223–237. [PubMed: 12687687]
7. Calvert GA. Crossmodal processing in the human brain: insights from functional neuroimaging studies. Cereb. Cortex 2001;11:1110–1123. [PubMed: 11709482]
8. Calvert GA, Bullmore ET, Brammer MJ, Campbell R, Williams SC, McGuire PK, Woodruff PW, Iversen SD, David AS. Activation of auditory cortex during silent lipreading. Science 1997;276:593–596. [PubMed: 9110978]
9. Driver J, Spence C. Multisensory perception: beyond modularity and convergence. Curr. Biol 2000;10:R731–R735. [PubMed: 11069095]
10. Ermentrout GB, Kleinfeld D. Traveling electrical waves in cortex: insights from phase dynamics and speculation on a computational role. Neuron 2001;29:33–44. [PubMed: 11182079]
11. Foxe JJ, Wylie GR, Martinez A, Schroeder CE, Javitt DC, Guilfoyle D, Ritter W, Murray MM. Auditory-somatosensory multisensory processing in auditory association cortex: an fMRI study. J. Neurophysiol 2002;88:540–543. [PubMed: 12091578]
12. Ghazanfar AA, Schroeder CE. Is neocortex essentially multisensory? Trends Cogn. Sci 2006;10:278–285. [PubMed: 16713325]
13. Giard MH, Peronnet F. Auditory-visual integration during multimodal object recognition in humans: a behavioral and electrophysiological study. J. Cogn. Neurosci 1999;11:473–490. [PubMed: 10511637]
14. Grinvald A, Arieli A, Tsodyks M, Kenet T. Neuronal assemblies: single cortical neurons are obedient members of a huge orchestra. Biopolymers 2003;68:422–436. [PubMed: 12601800]
15. Hoffer ZS, Hoover JE, Alloway KD. Sensorimotor corticocortical projections from rat barrel cortex have an anisotropic organization that facilitates integration of inputs from whiskers in the same row. J. Comp. Neurol 2003;466:525–544. [PubMed: 14566947]
16. Jones EG. Viewpoint: the core and matrix of thalamic organization. Neuroscience 1998;85:331–345. [PubMed: 9622234]
17. Kayser C, Petkov CI, Augath M, Logothetis NK. Integration of touch and sound in auditory cortex. Neuron 2005;48:373–384. [PubMed: 16242415]
18. Kenet T, Bibitchkov D, Tsodyks M, Grinvald A, Arieli A. Spontaneously emerging cortical representations of visual attributes. Nature 2003;425:954–956. [PubMed: 14586468]
19. Kleinfeld D, Delaney KR. Distributed representation of vibrissa movement in the upper layers of somatosensory cortex revealed with voltage-sensitive dyes. J. Comp. Neurol 1996;375:89–108. [PubMed: 8913895]
20. Laaris N, Keller A. Functional independence of layer IV barrels. J. Neurophysiol 2002;87:1028–1034. [PubMed: 11826066]

21. Lakatos P, Chen CM, O'Connell MN, Mills A, Schroeder CE. Neuronal oscillations and multisensory interaction in primary auditory cortex. Neuron 2007;53:279–292. [PubMed: 17224408]
22. Levanen S, Jousmaki V, Hari R. Vibration-induced auditory-cortex activation in a congenitally deaf adult. Curr. Biol 1998;8:869–872. [PubMed: 9705933]
23. Lippert MT, Takagaki K, Xu WF, Huang X, Wu JY. Methods for voltage-sensitive dye imaging of rodent cortical activity with high signal-to-noise ratio. J. Neurophysiol. 2007(in press)
24. Macaluso E, Frith CD, Driver J. Modulation of human visual cortex by crossmodal spatial attention. Science 2000;289:1206–1208. [PubMed: 10947990]
25. Menzel RR, Barth DS. Multisensory and secondary somatosensory cortex in the rat. Cereb. Cortex 2005;15:1690–1696. [PubMed: 15703251]
26. Miller MW, Vogt BA. Direct connections of rat visual cortex with sensory, motor, and association cortices. J. Comp. Neurol 1984;226:184–202. [PubMed: 6736299]
27. Molholm S, Ritter W, Murray MM, Javitt DC, Schroeder CE, Foxe JJ. Multisensory auditory-visual interactions during early sensory processing in humans: a high-density electrical mapping study. Brain Res.Cogn Brain Res 2002;14:115–128. [PubMed: 12063135]
28. Odgaard EC, Arieh Y, Marks LE. Brighter noise: sensory enhancement of perceived loudness by concurrent visual stimulation. Cogn. Affect. Behav. Neurosci 2004;4:127–132. [PubMed: 15460919]
29. Odgaard EC, Arieh Y, Marks LE. Cross-modal enhancement of perceived brightness: sensory interaction versus response bias. Percept. Psychophys 2003;65:123–132. [PubMed: 12699315]
30. Paperna T, Malach R. Patterns of sensory intermodality relationships in the cerebral cortex of the rat. J. Comp. Neurol 1991;308:432–456. [PubMed: 1865010]
31. Petersen CC, Grinvald A, Sakmann B. Spatiotemporal dynamics of sensory responses in layer 2/3 of rat barrel cortex measured in vivo by voltage-sensitive dye imaging combined with whole-cell voltage recordings and neuron reconstructions. J. Neurosci 2003;23:1298–1309. [PubMed: 12598618]
32. Petersen CC, Hahn TT, Mehta M, Grinvald A, Sakmann B. Interaction of sensory responses with spontaneous depolarization in layer 2/3 barrel cortex. Proc. Natl. Acad. Sci. U. S. A 2003;100:13638–13643. [PubMed: 14595013]
33. Peterson BE, Goldreich D, Merzenich MM. Optical imaging and electrophysiology of rat barrel cortex. I. Responses to small single-vibrissa deflections. Cereb. Cortex 1998;8:173–183. [PubMed: 9542896]
34. Roland PE, Hanazawa A, Undeman C, Eriksson D, Tompa T, Nakamura H, Valentiniene S, Ahmed B. Cortical feedback depolarization waves: a mechanism of top-down influence on early visual areas. Proc. Natl. Acad. Sci. U. S. A 2006;103:12586–12591. [PubMed: 16891418]
35. Schroeder CE, Foxe J. Multisensory contributions to low-level, 'unisensory' processing. Curr. Opin. Neurobiol 2005;15:454–458. [PubMed: 16019202]
36. Schroeder CE, Foxe JJ. The timing and laminar profile of converging inputs to multisensory areas of the macaque neocortex. Brain Res.Cogn Brain Res 2002;14:187–198. [PubMed: 12063142]
37. Schroeder CE, Lindsley RW, Specht C, Marcovici A, Smiley JF, Javitt DC. Somatosensory input to auditory association cortex in the macaque monkey. J. Neurophysiol 2001;85:1322–1327. [PubMed: 11248001]
38. Stein, BE.; Meredith, MA. The Merging of the Senses. MIT Press; 1993.
39. Tanifuji M, Sugiyama T, Murase K. Horizontal propagation of excitation in rat visual cortical slices revealed by optical imaging. Science 1994;266:1057–1059. [PubMed: 7973662]
40. Wallace MT, Ramachandran R, Stein BE. A revised view of sensory cortical parcellation. Proc. Natl. Acad. Sci. U. S. A 2004;101:2167–2172. [PubMed: 14766982]
41. Xu W, Huang X, Takagaki K, Wu JY. Compression and reflection of visually evoked cortical waves. Neuron 2007;55:119–129. [PubMed: 17610821]
42. Yazawa I, Sasaki S, Mochida H, Kamino K, Momose-Sato Y, Sato K. Developmental changes in trial-to-trial variations in whisker barrel responses studied using intrinsic optical imaging: comparison between normal and de-whiskered rats. J. Neurophysiol 2001;86:392–401. [PubMed: 11431519]

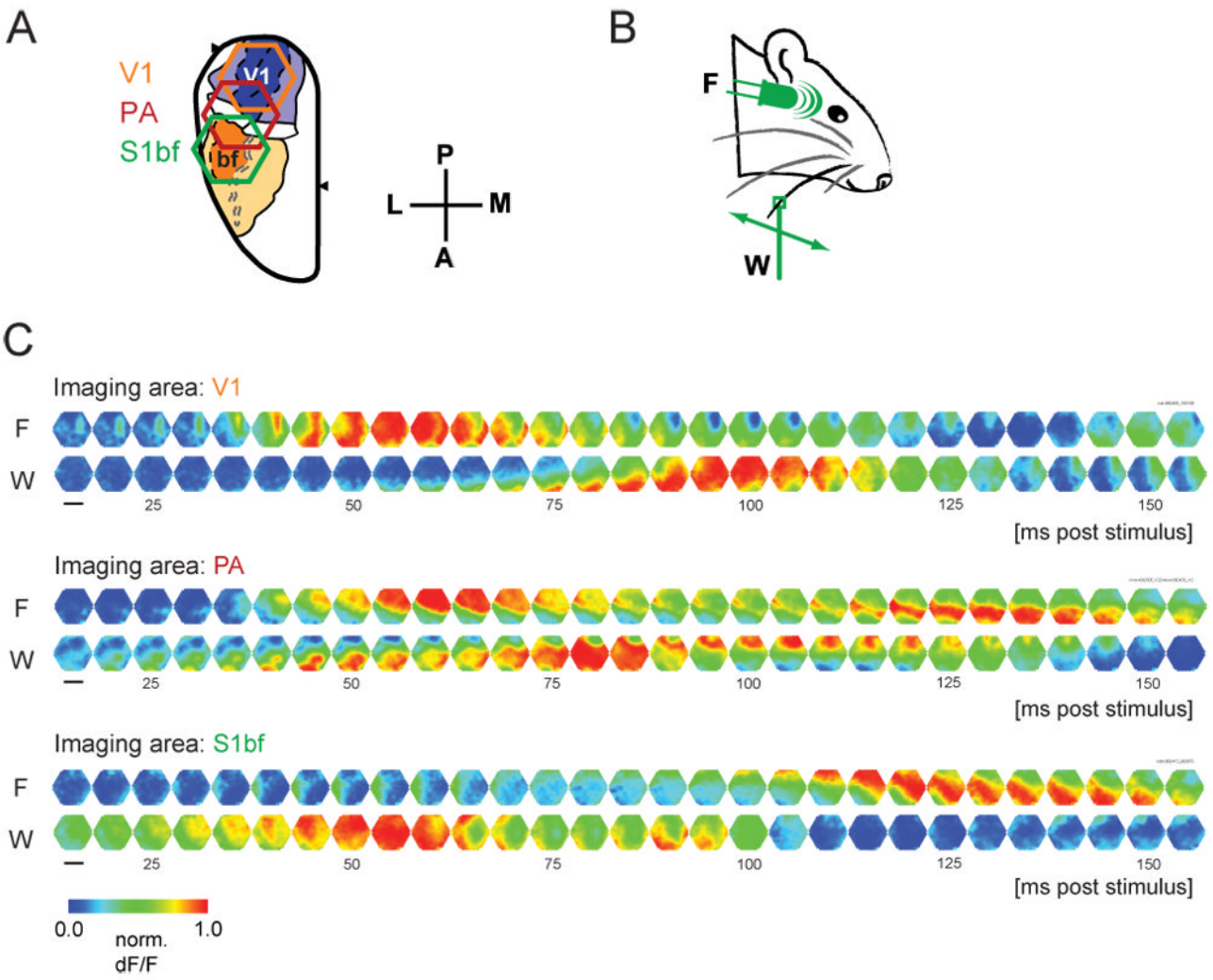

Figure 1. Examples of crossmodal propagation

A. Three hexagonal imaging fields, were positioned over V1 (orange), PA (red) or S1bf (green). The imaging apparatus consisted of a 464-channel photodiode array, and the imaging area was 10.4 mm^2. B. Sensory stimulus consisted of either a 10 ms white LED flash (F) or a 200 ms deflection of a single whisker in the anterior direction (W). C. Crossmodal propagation was observed in single trials in each area, but with varying latencies. Six representative single trials are shown. Sampling rate was 1.6 kHz, and one in every eight frames is displayed. Fluorescence changes in each trial were normalized to emphasize propagation patterns (scale bar, 2.0 mm).

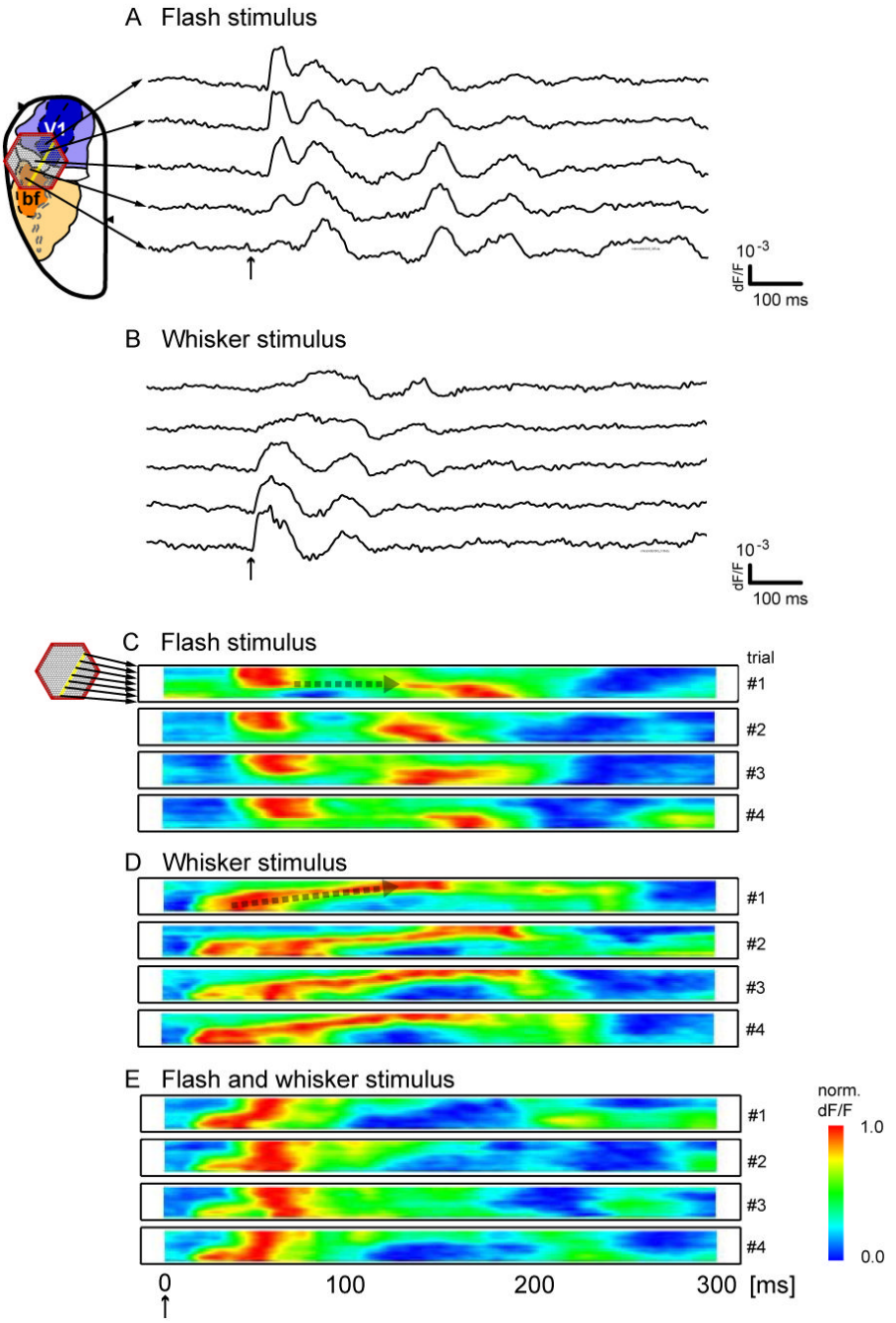

Figure 2. Variability in crossmodally propagating waveforms

A,B. Single-trial waveforms from five single detectors along the crossmodal propagation path (yellow dots) are displayed for single trials with flash stimulus (A) and whisker stimulus (B). Waveforms change continuously and dynamically as they propagate across the cortex, and their amplitudes do not diminish suddenly at areal borders. C, D, E. Linescans of four representative trials each, with either flash stimulus (C), whisker stimulus (D), or both (E). In each linescan, signal from all detectors highlighted in yellow were aligned along the ordinate. Each row of each linescan depicts the temporal evolution of the normalized signal from a single detector. Flash-evoked activity (C) propagates from the upper detectors in V1 towards the lower detectors in S1bf; whisker-evoked activity (D) propagates in the reverse direction.

Differences in onset and propagation pattern are seen in single trials. Simultaneous whisker and flash stimulation (E) leads to overall propagation from S1bf to V1; however, the spatiotemporal pattern is not a simple combination of those seen in C and D.

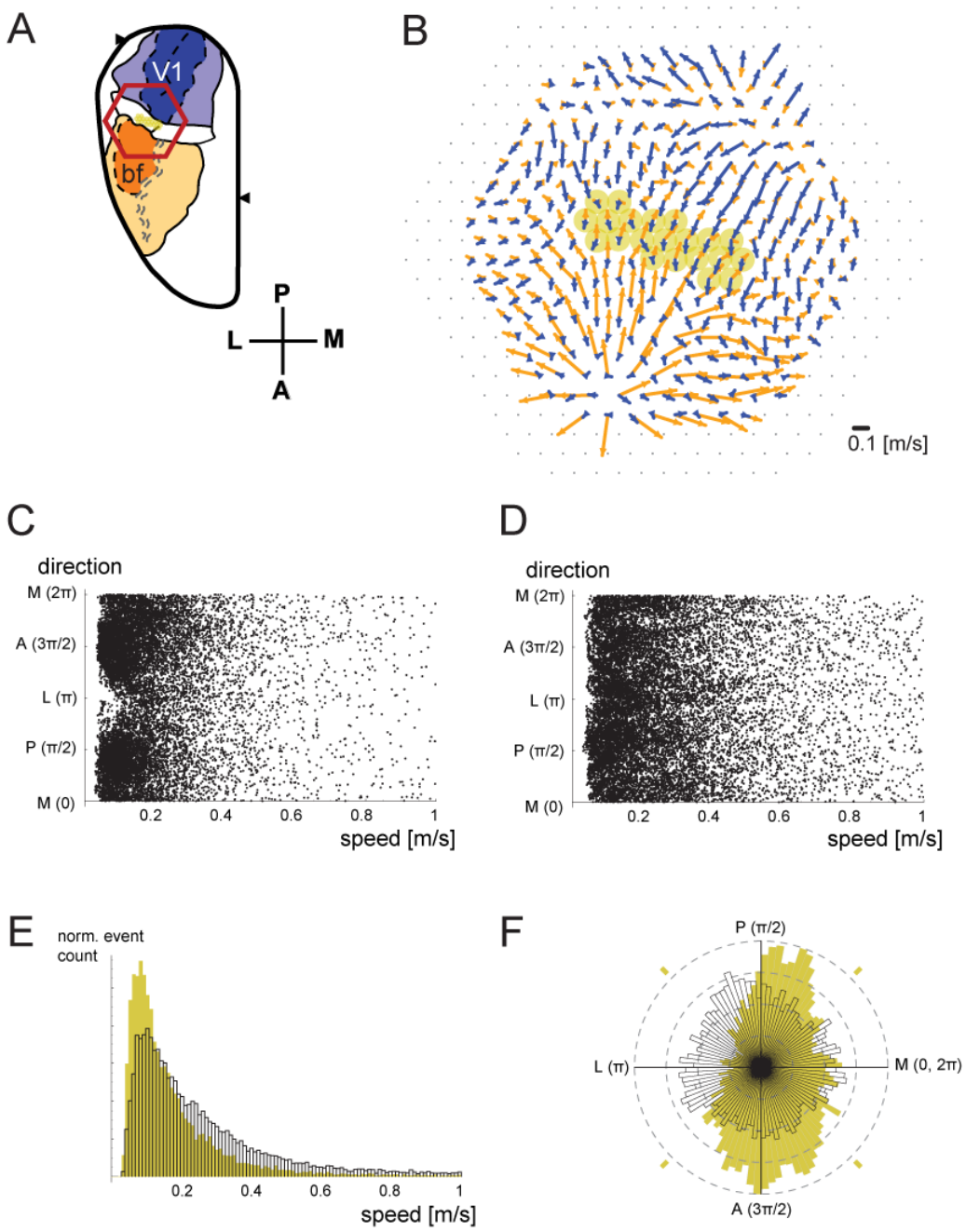

Figure 3. Crossmodal propagation preference of spontaneous waves

A. Imaging field for this figure. Selected detectors within PA are highlighted in yellow. B. The average crossmodal flow field in response to flash (blue) or whisker deflection (orange) was quantified, using the flow-detection algorithm described in the text (n=60 trials for each condition). Selected detectors from A are highlighted here as well. C. The flow of spontaneous events was detected using the same algorithm, at the detectors highlighted in A and B. Each dot represents a single flow event. Only flows with a reliability (mean correlation coefficient) higher than 0.9 were plotted. D. Similar analysis of data acquired from the center of the barrel cortex, around barrel C2. E. Normalized histograms of the event speeds of data in C and D. The data from panel C, which is from area PA, was plotted in yellow. The data from panel D,

from the center of S1bf, is plotted in white profile. F. Normalized rose histograms of the events are shown, in the same color scheme. Spontaneous events in PA (yellow) show a preference for the crossmodal direction, whereas those from the center of barrel cortex (white) do not.